JEMAT 2023, Vol 11, No 1, 1-9
https://doi.org/10.54987/jemat.v11i1.837

HIBISCUS PUBLISHER
JOURNAL OF ENVIRONMENTAL MICROBIOLOGY AND TOXICOLOGY
Website: http://journal.hibiscuspublisher.com/index.php/JEMAT/index

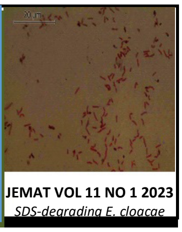

Isothermal Modelling of the Adsorption of Crystal violet onto Modified Charred Rice Husk

Bilal Ibrahim Dan-Iya[1], Mohd Ezuan Khayat[1] and Mohd Yunus Shukor[1]*

[1]Department of Biochemistry, Faculty of Biotechnology and Biomolecular Sciences, Universiti Putra Malaysia, 43400 UPM Serdang, Selangor, Malaysia.

*Corresponding author:
Mohd Yunus Shukor,
Department of Biochemistry,
Faculty of Biotechnology and Biomolecular Sciences,
Universiti Putra Malaysia,
43400 UPM Serdang,
Selangor,
Malaysia.
Email: mohdyunus@upm.edu.my

HISTORY

Received: 15th April 2023
Received in revised form: 23rd June 2023
Accepted: 19th July 2023

KEYWORDS

Biosorption
Crystal violet
Isotherm
Modified rice husk
Jovanovic isotherm

ABSTRACT

The rice milling process produces rice husk as a by-product. It is one of the most important agricultural leftovers in terms of volume. The data of the sorption isotherm of crystal violet (CV) sorption onto modified charred rice husk, which was plotted using linearized plots of isothermal models were reanalyzed using twenty isothermal models using nonlinear regression. Nineteen models — Henry, Langmuir, Freundlich, Jovanovic, Redlich-Peterson, Sips, Toth, Hill, Khan, BET, Vieth-Sladek, Radke-Prausnitz, Fritz-Schlunder III, Unilan, Baudu, Marczewski-Jaroniec, Fritz-Schluender IV, Weber-van Vliet and Fritz-Schluender V – fitted the data best using non-linear regression. Statistical analysis based on error function analyses such as root-mean-square error (RMSE), adjusted coefficient of determination (adjR^2), accuracy factor (AF), bias factor (BF), Bayesian Information Criterion (BIC), corrected AICc (Akaike Information Criterion), and Hannan-Quinn Criterion (HQC) showed that Jovanovic model was the best model. The maximal adsorption capacity in the Jovanovic model, expressed in milligrams per gram (mg/g), is denoted by q_{mJ} while K_j is the Jovanovic constant, and the calculated values were 55.979 mg/L (95% confidence interval; 52.556 to 59.403) and 0.010 (95% confidence interval; 0.008 to 0.012), respectively. The nonlinear regression method provides parameter values within the 95% confidence interval, facilitating improved comparability with prior research.

INTRODUCTION

Dye users provide color to textiles, paper, leather, and other materials to beautify and preserve them, therefore the environmental pollution and health risks of dye contamination are of great concern in nearly all nations in the developing world [1]. A dye is a powdered material that is mixed with another product or dissolved in a liquid (like paint or ink). Pigments are dispersed solids that are often powdered [2]. Both natural and synthetic dyes see extensive use because to their decorative and protective qualities. Once easily extracted from their complex mixtures, natural dyes are now notoriously finicky and time-consuming to isolate. These hues also inspired the development of modern synthetic dyes. Dyes are unique among organic compounds in that they absorb light in the visible spectrum due to their conjugated structure, chromophores, and absorbing chromophores [3]. It is a significant difficulty to remove color from wastewater containing dyes using conventional treatment methods. Fish and other aquatic organisms are put at risk by the toxic organic compounds found in the wastewater discharged into rivers during the dye manufacturing and textile finishing processes [4]. Dyestuffs, textiles, paper, and plastics are just a few examples of sectors that rely on color. They create significant quantities of colored effluent byproducts, which eventually drain into water sources [3]. Such technological advances in industry, whether deliberate or accidental, have contributed to rising pollution levels as cities and populations have expanded. In order to prevent the release of industry waste effluents into the environment, textile companies must treat their effluents before releasing them [5]. When water is contaminated by synthetic color molecules, it has negative effects on both the environment and human health.

Dye runoff contributes to eutrophication and is a kind of aesthetic pollution. Textiles, leather, paper, paint, acrylic, cosmetics, plastic, medications, and other products that rely on dyes to provide color are essential to society. They drink a lot of water as well [6]. This results in copious volumes of discolored wastewater. Therefore, this research was carried out to lessen the prevalence of potentially harmful color pollution in potable water.

Wastewater cannot be discharged until all dyes have been removed. Chemical oxidation using chlorine and ozone, and adsorption techniques using alum, lime, ferric sulfate, and ferric chloride are also viable options [7,8], membrane separation processes [9,10], and adsorption [9,10]. The most promising therapies appear to be those based on adsorption. Recent years have seen a rise in the use of physicochemical methods including adsorption and electrochemical coagulation. Adsorption's convenience and versatility have contributed to its rising popularity [11,12].

Biological degradation, membrane filtration, and ion exchange are some more options besides oxidation by ozone or hydrogen peroxide [13,14], electrochemical oxidation [13], reverse osmosis [15], photocatalytic degradation [15], and adsorption [15], Dye removal has been attempted using a number of various methods. There is a wide range of strategies for removing colors, each with its own cost in time and money.

The equilibrium, kinetic, and thermodynamic aspects of CV dye adsorption on modified rice husk (NMRH) were studied by Chakraborty et al. in 2011 [16]. The adsorption of CV dye on chemically modified rice husk (CMRH) was also the subject of an experimental batch research by Das et al. in 2012 [17]. The CMRH adsorbent was the most effective.

To remove the CV dye from water, adsorbent nanoparticles containing rice husk (TARH) were utilized [18]. An improved magnetic biochar nanocomposite (MBC) was developed by combining rice husk and iron oxide nanoparticles (IONPs), and its efficacy in either reducing CV dye in aqueous solutions or completely removing it was evaluated [19]. The effectiveness of NaOH-modified rice husk in adsorbing CV dye from aqueous solution was evaluated in laboratory-scale fixed-bed columns [20]. It has been discovered that RHC can absorb CV color from water [3].

In one experiment, bio-nanosilica was extracted from rice husk using ultrasonic technology, and CV dye was adsorbed onto aqueous effluents [21]. In order to remove the colour from the water, rice husk (RH) was utilized. Z-RHA, or zeolites mediated by rice husk ash, were created by a chemical alteration, and studies comparing their efficacy in cleaning up CV dye-tainted water were carried out [22]. According to the literature [11], Using RH as an adsorbent, which was easily accessible and cheap, CV could be removed from wastewater. RHC was also used to eliminate the CV dye.

The effects of other variables, such as agitation time, pH, and adsorbent concentration, have also been investigated [3]. Succinic acid-treated rice husk has been found to be effective at bleaching aqueous solutions [23]. The adsorption pattern of CV dye on succinic acid-treated rice husk was also assessed using a cyclic voltammetry method. Because of this, the oxidation and reduction signal both got bigger, and an oxidation peak showed up.

In order to get rid of CV dye in water, Van Hung synthesized nanosilica from rice husk [3]. The rice husk was "turned on" with nitric acid. Crystal violet-containing wastewater adsorption capacity was evaluated [24]. CV dye was shown to be effectively removed from aqueous solutions by using rice husk, sodium carbonate, and potassium hydrogen phosphate. Raw rice husk (RRH) is not an effective biosorbent since the process of dye adsorption onto it increases the chemical oxygen demand (COD) of the treated effluent. They also remove colors from treated wastewater while decreasing COD. A chemical oxygen demand (COD) analysis should be done to evaluate the biosorbent [3].

Crystal violet, like many other synthetic hues, is not biodegradable, is toxic, causes mutations and cancer, and can trigger allergies and skin rashes even in minute doses. Crystal violet can cause stomach upset, diarrhea, and gastritis if taken orally. Ingestion of large quantities can lead to nausea, abdominal pain, vomiting, severe headaches, chest pain, profuse sweating, confusion, painful urination, and hemoglobinemia. Crystal violet is toxic if ingested and can cause nausea, vomiting, and diarrhea if inhaled. Mucous membrane and gastrointestinal tract damage can occur with prolonged exposure [25].

Accurate assignment of adsorption kinetics and isotherms is essential for understanding the adsorption process in this context. The clearly nonlinear curve in this data is often presented in the literature with a linearized form. Because the error structure of the data changes when nonlinear data is linearized, estimating uncertainty is more challenging [26]. In this study, the published data from Chrystal violet dye adsorption onto charred rice husk was modelled with various isothermal models (**Table 1**) as well as regressed by the method of nonlinear regression. Best-fitted isotherm assessment was conducted using several error function analyses.

METHOD

Data acquisition and fitting

Figure 7 data from a previously published study [3] was digitized using the freeware Webplotdigitizer 2.5 [27]. After that, the data were nonlinearly regressed using the curve-fitting program Curve-Expert Professional (Version 1.6). Digitization using this program has been praised for its dependability [28,29].

Statistical analysis

A set of statistical discriminatory tests such as corrected AICc (Akaike Information Criterion), Bayesian Information Criterion (BIC), Hannan and Quinn's Criterion (HQ), Root-Mean-Square Error (RMSE), bias factor (BF), accuracy factor (AF) and adjusted coefficient of determination (R^2) were used in this study.

Table 1. Mathematical models that were used in modelling data [30,31].

Isotherm	p	Formula	Ref.
Henry's law	1	$q_e = HC_e$	[32]
Langmuir	2	$q_e = \frac{q_{mL} b_L C_e}{1 + b_L C_e}$	[30]
Jovanovic	2	$q_e = q_{mJ}(1 - e^{-K_j C_e})$	[33]
Freundlich	2	$q_e = K_F C_e^{\frac{1}{n_F}}$	[34]
Temkin	3	$q_e = \frac{RT}{b_T}\{ln(a_T C_e)\}$	[35]
Dubinin-Radushkevich	2	$q_e = q_{mDR} exp\left\{-K_{DR}\left[RT ln\left(1 + \frac{1}{C_e}\right)\right]^2\right\}$	[36,37]
Redlich-Peterson	3	$q_e = \frac{K_{RP1} C_e}{1 + K_{RP2} C_e^{\beta_{RP}}}$	[38]
Sips	3	$q_e = \frac{K_s q_{mS} C_e^{\frac{1}{n_S}}}{1 + K_s C_e^{\frac{1}{n_S}}}$	[39]
Toth	3	$q_e = \frac{q_{mT} C_e}{\left(K_T + C_e^{n_T}\right)^{n_T}}$	[40]
Hill	3	$q_e = \frac{q_{mH} C_e^{n_H}}{K_H + C_e^{n_H}}$	[9]
Khan	3	$q_e = \frac{q_{mK} b_K C_e}{(1 + b_K C_e)^{a_K}}$	[41]
BET	3	$q_e = \frac{q_{mBET} \alpha_{BET} C_e}{(1 - \beta_{BET} C_e)(1 - \beta_{BET} C_e + \alpha_{BET} C_e)}$	[42]
Vieth-Sladek	3	$q_e = \frac{q_{mVS} b_{VS} C_e}{(1 + b_{VS} C_e)^{n_{VS}}}$	[43]
Radke-Prausnitz	3	$q_e = \frac{q_{mRP} K_{RP} C_e}{(1 + K_{RP} C_e)^{n_{RP}}}$	[44]
Brouers–Sotolongo	3	$q_e = q_{mBS}\left(-K_{BS} C_e^{n_{BS}}\right)$	[45]
Fritz-Schlunder-III	3	$q_e = \frac{q_{mFS} K_{FS} C_e}{1 + K_{FS} C_e^{n_{FS}}}$	[46]
Unilan	3	$q_e = \frac{q_{mU}}{2b_U} ln\left(\frac{a_U + C_e e^{b_U}}{a_U + C_e e^{-b_U}}\right)$	[15]
Baudu	4	$q_e = \frac{q_{mB} b_B C_e^{(1+x+y)}}{1 + b_B C_e^{(1+x)}}$	[47]
Marczewski-Jaroniec	4	$q_e = q_{mMJ}\left(\frac{\left(K_{MJ} C_e\right)^{n_{MJ}}}{1 + \left(K_{MJ} C_e\right)^{n_{MJ}}}\right)^{\frac{m_{MJ}}{n_{MJ}}}$	[48]
Fritz-Schlunder-IV	4	$q_e = \frac{A_{FS} C_e^{a_{FS}}}{1 + B_{FS} C_e^{b_{FS}}}$	[46]
Weber-van Vliet	4	$C_e = P_1 q_e^{\left(P_2 q_e^{P_3} + P_4\right)}$	[49]
Fritz-Schlunder-V	5	$q_e = \frac{q_{mFS5} K_1 C_e^{\alpha_{FS}}}{1 + K_2 C_e^{\beta_{FS}}}$	[46]

The RMSE was computed using Equation 1, and it stands to reason that the fewer parameters utilized, the smaller the RMSE will be. n is for the total number of observations made in the experiment, Obi and Pdi stand for the total number of observations made in the experiment and projections, and p stands for the total number of parameters [26] .

$$RMSE = \sqrt{\frac{\sum_{i=1}^{n}(Pd_i - Ob_i)^2}{n-p}} \qquad \text{(Eqn. 1)}$$

Because R^2 or the coefficient of determination ignores the number of parameters in a model, the modified R^2 is used to overcome this limitation. The entire variance of the y-variable is given by $S^2{}_y$ in the equation (**Equations 2** and **3**), while RMS is the Residual Mean Square.

$$Bias\ factor = 10\left(\sum_{i=1}^{n} log \frac{(Pd_i/Ob_i)}{n}\right) \qquad \text{(Eqn. 2)}$$

$$Accuracy\ factor = 10\left(\sum_{i=1}^{n} log \frac{|(Pd_i/Ob_i)|}{n}\right) \qquad \text{(Eqn. 3)}$$

The AICc is computed as follows (**Equation 4**), where p represents the number of parameters and n represents the number of data points. The corrected Akaike information criterion (AICc) is used to manage data with a large number of parameters but a limited number of values [50]. A model with a lower AICc score is considered more likely to be right [50]. The information theory is the foundation of the Akaike Information Criterion (AIC). It strikes a compromise between the goodness of fit of a given model and the model's complexity [51].

$$AICc = 2p + n\ln\left(\frac{RSS}{n}\right) + \frac{2(p+1)+2(p+2)}{n-p-2} \qquad \text{(Eqn. 4)}$$

Another statistical tool based on information theory apart from AICc, is the Bayesian Information Criterion (BIC) (Equation 5). The number of parameters is penalized more severely by this error function than by AIC [27].

$$BIC = n\ln\left(\frac{RSS}{n}\right) + k\ln(n) \qquad \text{(Eqn. 5)}$$

The Hannan-Quinn information criterion (HQC) (**Equation 6**) is another error function approach based on information theory. Because of the ln ln n element in the calculation, the HQC is more consistent than the AIC [50].

$$HQC = nln\left(\frac{RSS}{n}\right) + 2k\ln(\ln n) \qquad \text{(Eqn. 6)}$$

The Accuracy Factor (AF) and Bias Factor (BF) are two further error function analyses derived from Ross's work [50]. These error functions evaluate models statistically for goodness-of-fit but do not penalize for the number of parameters (**Equations 7** and **8**).

$$Adjusted\ (R^2) = 1 - \frac{RMS}{S_Y^2} \qquad \text{(Eqn. 4)}$$

$$Adjusted\ (R^2) = 1 - \frac{(1-R^2)(n-1)}{(n-p-1)} \qquad \text{(Eqn. 5)}$$

RESULTS AND DISCUSSION

The equilibrium data from [3] was analyzed using fifteen models—Henry, Langmuir, Freundlich, Redlich-Petersen, Sips, BET, Toth, Hill, Khan, Vieth-Sladek, Radke-Prausnitz, Unilan, Fritz-Schlunder III, Fritz-Schlunder IV, and Fritz-Schlunder V, were used in finding the best fit by utilizing non-linear regression. Henry, Langmuir, Hill, Vieth-Sladek, Unilan, Sips and BET does not fit well with the data, whereas Freundlich, Redlich-Petersen, Toth, Khan, Radke-Prausnitz, Fritz-Schlunder III, Fritz-Schlunder IV, and Fritz-Schlunder V, fitted well with the data (**Figs. 1 – 19**).

The best isotherm model was found to be the Jovanovic with the lowest RMSE and AF, BF and adjR^2 values closest to unity and lowest BIC, HQC and AICc values followed (descending order) by Langmuir, Sips, Hill and Redlich-Petersen (**Table 2**). As enough models fitted well with the charred rice husk data, it explains and justifies the more accuracy of using nonlinear regression as against the linear regression used in the original publication which suggests the 2-parameter Jovanovic isotherm as the best model.

https://doi.org/10.54987/jemat.v11i1.837

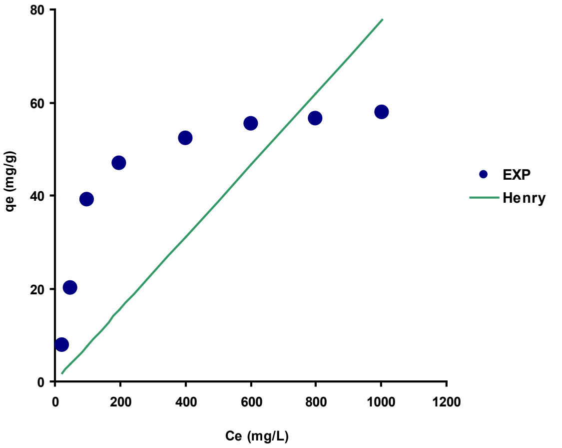

Fig. 1. Adsorption isotherm of crystal violet onto modified charred rice husk as modelled using the Henry model.

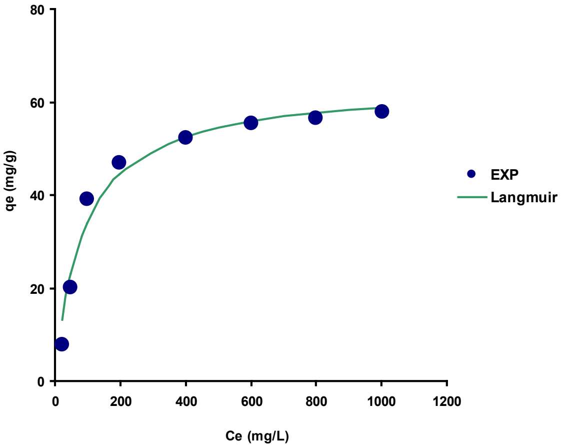

Fig. 2. Adsorption isotherm of crystal violet onto modified charred rice husk as modelled using the Langmuir isotherm model.

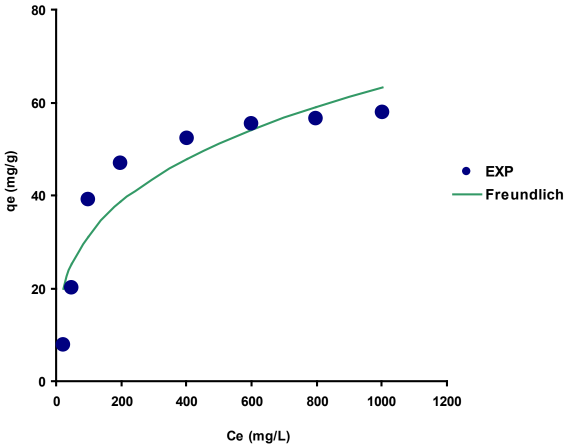

Fig. 3. Adsorption isotherm of crystal violet onto modified charred rice husk as modelled using the Freundlich isotherm model.

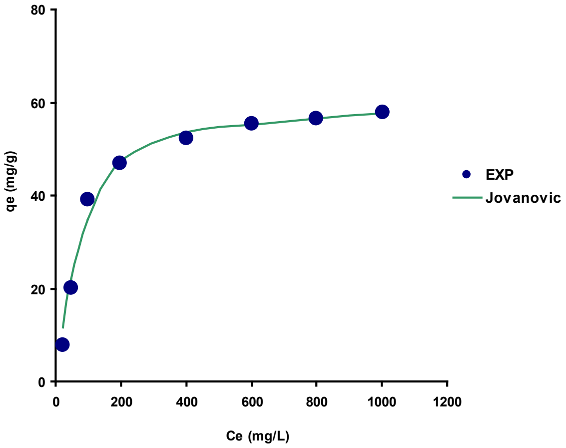

Fig. 4. Adsorption isotherm of crystal violet onto modified charred rice husk as modelled using the Jovanovic isotherm model.

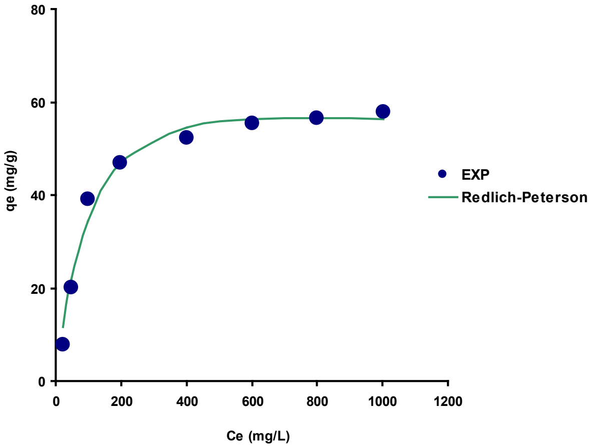

Fig. 5. Adsorption isotherm of crystal violet onto modified charred rice husk as modelled using the Redlich-Peterson isotherm model.

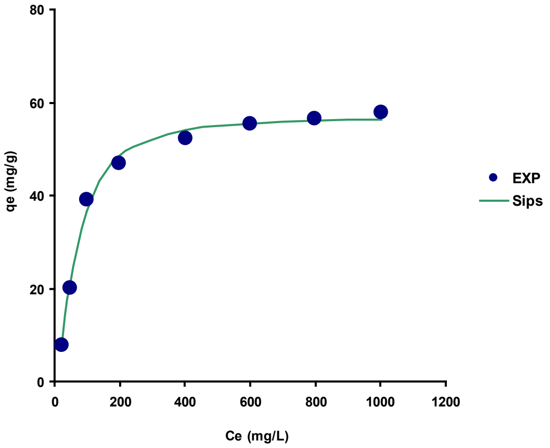

Fig. 6. Adsorption isotherm of crystal violet onto modified charred rice husk as modelled using the Sips isotherm model.

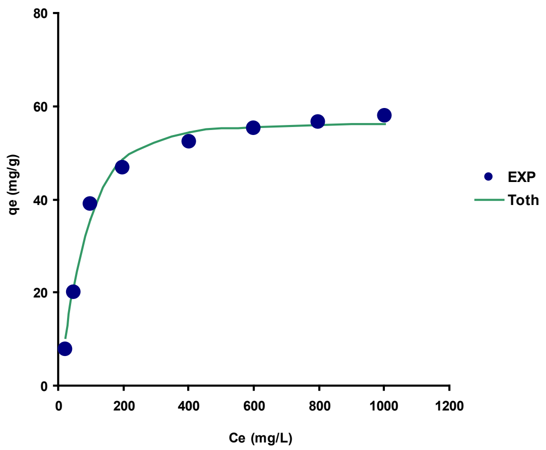

Fig. 7. Adsorption isotherm of crystal violet onto modified charred rice husk as modelled using the Toth isotherm model.

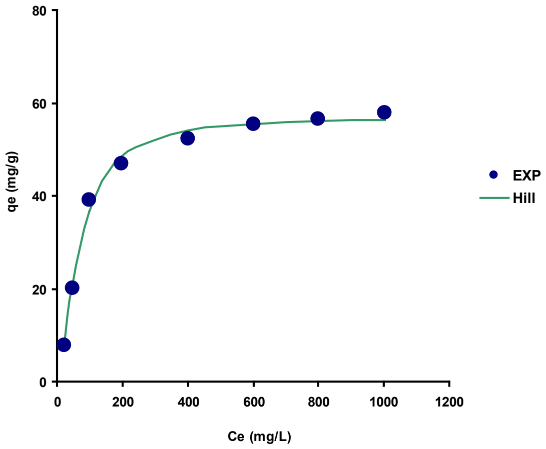

Fig. 8. Adsorption isotherm of crystal violet onto modified charred rice husk as modelled using the Hill isotherm model.

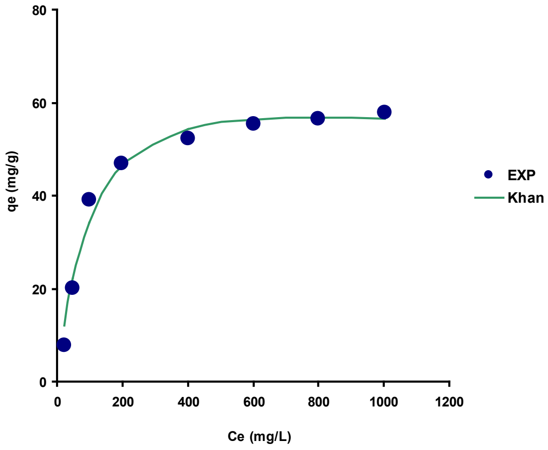

Fig. 9. Adsorption isotherm of crystal violet onto modified charred rice husk as modelled using the Khan isotherm model.

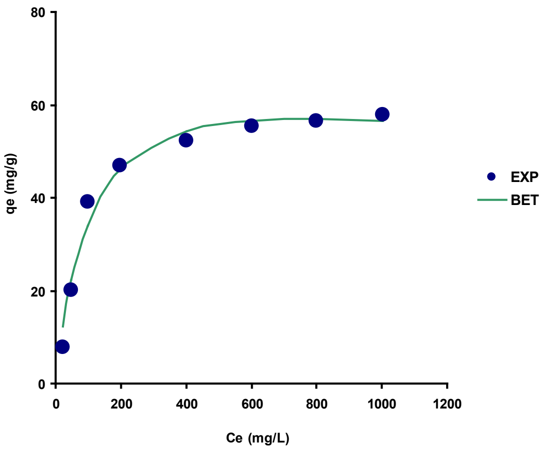

Fig. 10. Adsorption isotherm of crystal violet onto modified charred rice husk as modelled using the BET isotherm model.

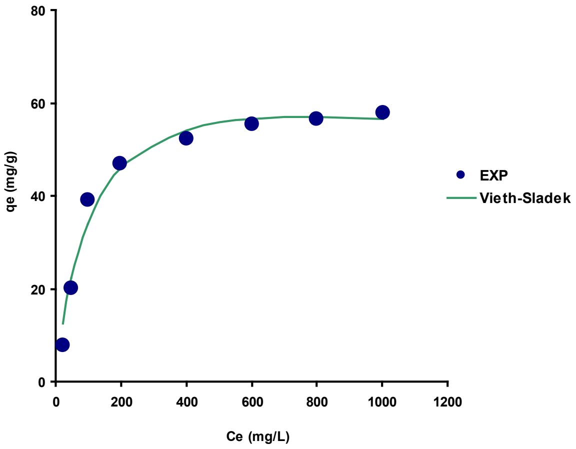

Fig. 11. Adsorption isotherm of crystal violet onto modified charred rice husk as modelled using the Vieth-Sladek isotherm model.

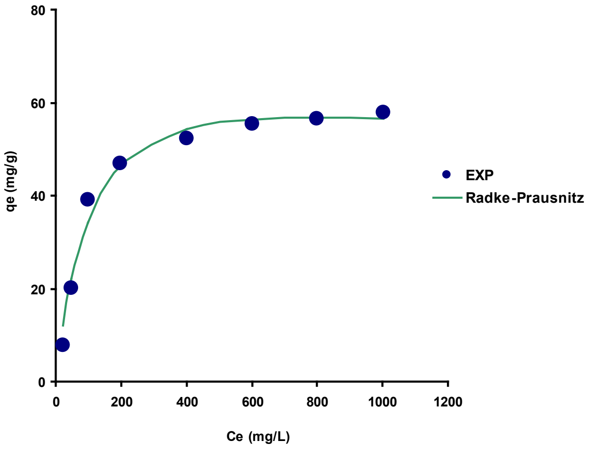

Fig. 12. Adsorption isotherm of crystal violet onto modified charred rice husk as modelled using the Radke-Prausnitz isotherm model.

https://doi.org/10.54987/jemat.v11i1.837

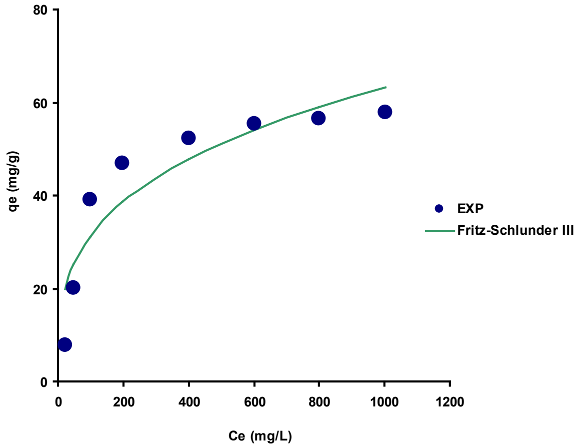

Fig. 13. Adsorption isotherm of crystal violet onto modified charred rice husk as modelled using the Fritz-Schlunder III isotherm model.

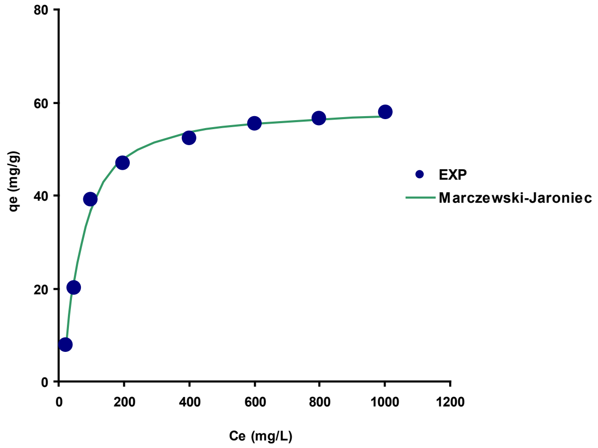

Fig. 16. Adsorption isotherm of crystal violet onto modified charred rice husk as modelled using the Marczewski-Jaroniec isotherm model.

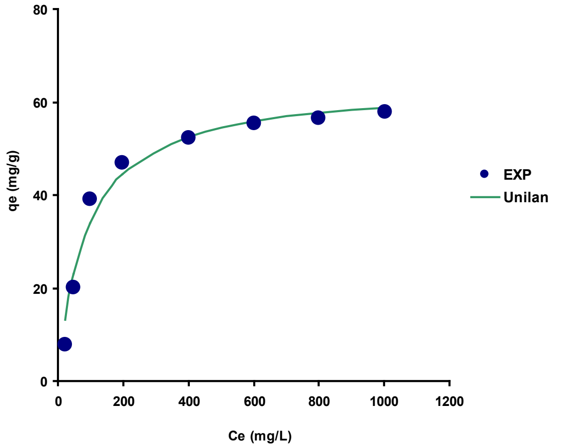

Fig. 14. Adsorption isotherm of crystal violet onto modified charred rice husk as modelled using the Unilan isotherm model.

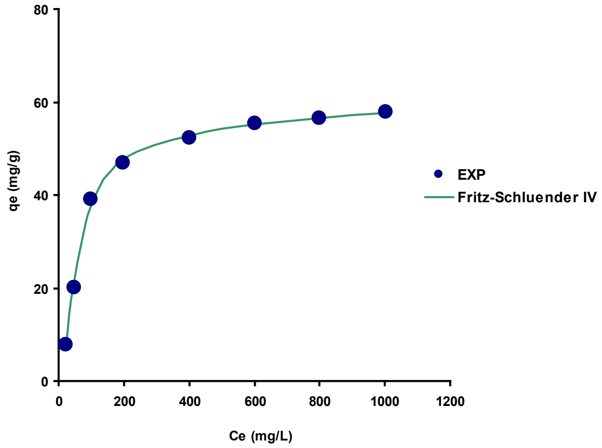

Fig. 17. Adsorption isotherm of crystal violet onto modified charred rice husk as modelled using the Fritz-Schluender IV isotherm model.

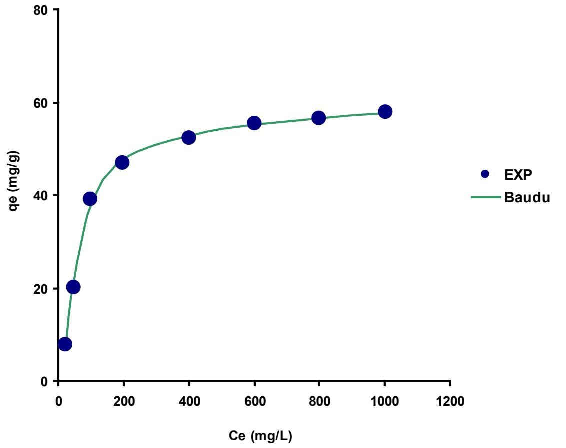

Fig. 15. Adsorption isotherm of crystal violet onto modified charred rice husk as modelled using the Baudu isotherm model.

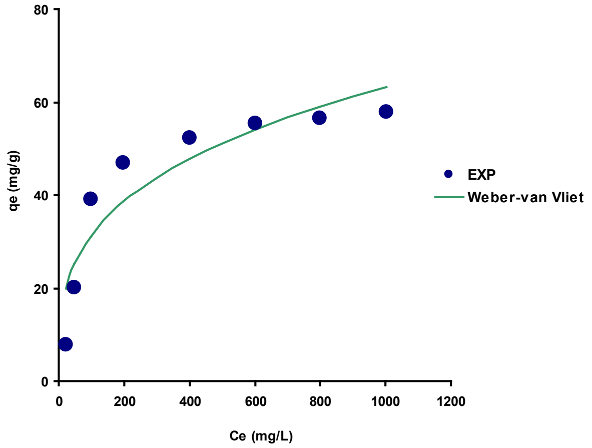

Fig. 18. Adsorption isotherm of crystal violet onto modified charred rice husk as modelled using the Weber-van Vliet isotherm model.

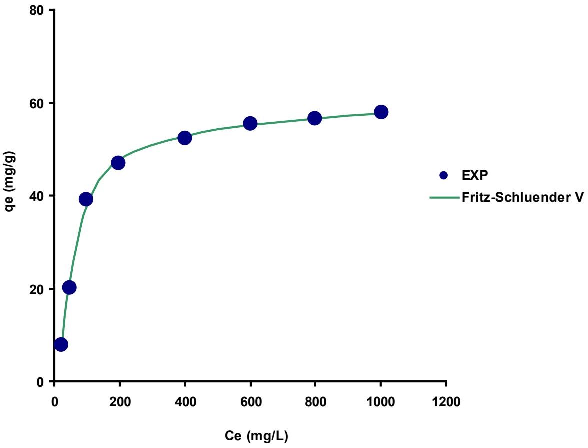

Fig. 19. Adsorption isotherm of crystal violet onto modified charred rice husk as modelled using the Fritz-Schluender V isotherm model.

Table 2. Error function analysis for the fitting of the isotherm of crystal violet onto modified charred rice husk.

Model	*p*	*RMSE*	*adR²*	*AICc*	*BIC*	*HQC*	*BF*	*AF*
Henry	1	21.500	0.35	56.42	56.4	50.1	0.53	1.89
Langmuir	2	3.493	0.95	33.71	33.7	21.87	0.99	1.04
Freundlich	2	7.765	0.72	46.49	46.5	34.65	0.96	1.10
Temkin	2	n.a.	n.a.	n.a.	n.a.	n.a.	n.a.	n.a.
Dubinin-Radushkevich	2	n.a.	n.a.	n.a.	n.a.	n.a.	n.a.	n.a.
Jovanovic	2	2.486	0.98	28.27	28.3	16.43	1.00	1.03
Redlich-Peterson	2	2.829	0.97	30.34	30.3	18.5	1.00	1.04
Sips	3	1.705	0.99	32.11	32.1	11.02	1.01	1.02
Toth	3	2.380	0.98	37.44	37.4	16.35	1.01	1.03
Hill	3	1.705	0.99	32.11	32.1	11.02	1.01	1.02
Khan	3	3.276	0.92	42.56	42.6	21.46	1.00	1.04
BET	3	3.437	0.95	43.33	43.3	22.23	1.00	1.04
Vieth-Sladek	3	3.476	0.95	43.51	43.5	22.41	1.00	1.04
Radke-Prausnitz	3	3.276	0.96	42.56	42.6	21.46	1.00	1.04
Brouers–Sotolongo	3	n.a.	n.a.	n.a.	n.a.	n.a.	n.a.	n.a.
Fritz-Schlunder III	3	8.506	0.65	57.83	57.8	36.73	0.96	1.10
Unilan	3	3.838	0.94	45.09	45.1	24	0.99	1.04
Baudu	4	1.220	0.99	45.64	45.6	5.96	1.01	1.02
Marczewski-Jaroniec	4	1.695	0.99	50.90	50.9	11.21	1.01	1.02
Fritz-Schluender IV	4	1.221	0.99	45.65	45.7	5.97	1.01	1.02
Weber-van Vliet	4	9.510	0.54	78.49	78.5	38.81	0.96	1.10
Fritz-Schluender V	5	1.410	0.99	103.65	103.7	8.05	1.01	1.02

Note:

RMSE	Root mean Square Error
adR²	Adjusted Coefficient of determination
p	no of parameters
AF	Accuracy factor
BF	Bias factor
BIC	Bayesian Information Criterion
AICc	Adjusted Akaike Information Criterion
HQC	Hannan–Quinn information criterion

The Jovanovic isotherm considers an adsorption surface assumption, which is similar to the Langmuir's. A second approximation for localized monolayer adsorption in the absence of lateral interactions corresponds to this scenario. The main distinction between this model and the Langmuir model is that the surface binding vibrations of an adsorbed species are considered [33].

The maximal adsorption capacity in the Jovanovic model, expressed in milligrams per gram (mg/g), is denoted by q_{mJ} while K_j is the Jovanovic constant, and the calculated values were 55.979 mg/L (95% confidence interval; 52.556 to 59.403) and 0.010 (95% confidence interval; 0.008 to 0.012), respectively (**Table 3**). The isotherm additionally considers the surface binding vibrations of the adsorbed species. A 3-parameter Jovanovic isotherm is also available and considers multilayer adsorption [33].

Table 3. Isothermal models' constants for the TB dye adsorption using *Pseudomonas* sp. strain MM02.

Model	*p*	Unit	Value	(95% confidence interval)
Langmuir	q_{mL}	mg g^{-1}	63.889	57.055 to 70.723
	b_L	L mg^{-1}	0.012	0.006 to 0.017
Jovanovic	q_{mJ}	mg g^{-1}	55.979	52.556 to 59.403
	K_J	dimensionless	0.010	0.008 to 0.012
Redlich – Peterson	K_{RP1}	L mg^{-1}	0.003	-0.004 to 0.011
	β_{RP}	dimensionless	1.147	0.875 to 1.419
	K_{RP2}	L g^{-1}	0.577	0.297 to 0.856
Sips	q_{mS}	mg g^{-1}	57.089	54.037 to 60.140
	K_S	L g^{1}	0.001	-0.001 to 0.003
	n_S	dimensionless	0.613	0.462 to 0.765
Hill isotherm	q_{mH}	mg g^{-1}	57.089	54.037 to 60.140
	n_H	dimensionless	1.63	1.228 to 2.033
	K_H	dimensionless	980.2	-617.9 to 2578.3

Note
*Isotherm with ln term should not be plotted using data that starts from the origin (0,0)
‡Isotherms having an RT term should be plotted using the temperature (Kelvin) studied

Dye, effluent, and trace element removal from wastewater can be accomplished using a variety of sorbents prepared by coating, chemical synthesis, and other methods [46–51]. Rice husk is a waste product created during the milling of rice. In terms of total volume, it is among the most significant agricultural byproducts. It's responsible for about 20% of the total rice output in some nations, including Egypt [52,53]. It is estimated that developing countries would produce 500 million tons of rice each year, with around 100 million tons of rice husk available for utilization. Historically, rice husks have been employed not only by the rice industry as a fuel source for boilers, but also in the production of blocks used in civil construction as panels [53,54]. However, there are many more rice husks available that can be used locally, leading to disposal problems. The granular structure, chemical stability, and inexpensive production costs of this material led to its selection, as did the fact that it does not require regeneration.

CONCLUSION

Finally, multiple models with one to five parameters have been fitted using non-linear regression to the adsorption isotherm data of crystal violet dye onto modified charred rice husk. Root-mean-square error (RMSE), adjusted coefficient of determination (*adjR²*), bias factor (BF), accuracy factor (AF), bias information coefficient (BIC), and the corrected Akaike Information Criterion (AICc) all indicate that the showed that the Fritz-Schlunder IV model was the best model in terms of overall best criteria. The maximal adsorption capacity in the Jovanovic model, expressed in milligrams per gram (mg/g), is denoted by q_{mJ} while K_j is the Jovanovic constant, and the calculated values were 55.979 mg/L (95% confidence interval; 52.556 to 59.403) and 0.010 (95% confidence interval; 0.008 to 0.012), respectively. The nonlinear regression approach represents parameter values in the 95% confidence interval range, which allows for better comparison with published findings.

REFERENCES

1. Lellis B, Fávaro-Polonio CZ, Pamphile JA, Polonio JC. Effects of textile dyes on health and the environment and bioremediation potential of living organisms. Biotechnol Res Innov. 2019;3(2):275–90.
2. Hielscher K. Ultrasonic Milling and Dispersing Technology for Nano-Particles. MRS Online Proc Libr. 2012;1479(1):21–6.
3. Homagai PL, Poudel R, Poudel S, Bhattarai A. Adsorption and removal of crystal violet dye from aqueous solution by modified rice husk. Heliyon. 2022;8(4):e09261.
4. Zabłocka-Godlewska E, Przystaś W, Grabińska-Sota E. Possibilities of Obtaining from Highly Polluted Environments: New Bacterial Strains with a Significant Decolorization Potential of Different Synthetic Dyes. Water Air Soil Pollut. 2018;229(6).
5. Slama H Ben, Bouket AC, Pourhassan Z, Alenezi FN, Silini A, Cherif-Silini H, et al. Diversity of synthetic dyes from textile industries, discharge impacts and treatment methods. Appl Sci Switz. 2021;11(14):1–21.
6. Khattab TA, Abdelrahman MS, Rehan M. Textile dyeing industry: environmental impacts and remediation. Environ Sci Pollut Res. 2020;27(4):3803–18.
7. Thamaraiselvan C, Noel M. Membrane processes for dye wastewater treatment: Recent progress in fouling control. Crit Rev Environ Sci Technol. 2015;45(10):1007–40.
8. Brik M, Chamam B, Schöberl P, Braun R, Fuchs W. Effect of ozone, chlorine and hydrogen peroxide on the elimination of colour in treated textile wastewater by MBR. Water Sci Technol. 2004;49(4):299–303.
9. Sivalingam S, Sen S. Rice husk ash derived nanocrystalline ZSM-5 for highly efficient removal of a toxic textile dye. J Mater Res Technol. 2020;9(6):14853–64.
10. Mohanty K, Naidu JT, Meikap BC, Biswas MN. Removal of crystal violet from wastewater by activated carbons prepared from rice husk. Ind Eng Chem Res. 2006;45(14):5165–71.
11. Quansah JO, Hlaing T, Lyonga FN, Kyi PP, Hong SH, Lee CG, et al. Nascent rice husk as an adsorbent for removing cationic dyes from textile wastewater. Appl Sci Switz. 2020;10(10).
12. Persulfate B activated, Avramiotis E, Frontistis Z, Manariotis ID, Vakros J, Mantzavinos D. Oxidation of Sulfamethoxazole by Rice Husk. 2021;
13. Sala M, Gutiérrez-Bouzán MC. Electrochemical techniques in textile processes and wastewater treatment. Int J Photoenergy. 2012;2012.
14. Karcher S, Kornmüller A, Jekel M. Anion exchange resins for removal of reactive dyes from textile wastewaters. Water Res. 2002;36(19):4717–24.
15. Abid MF, Zablouk MA, Abid-Alameer AM. Experimental study of dye removal from industrial wastewater by membrane technologies of reverse osmosis and nanofiltration. J Environ Health Sci Eng. 2012;9(1):1–9.
16. Chakraborty S, Chowdhury S, Das Saha P. Adsorption of Crystal Violet from aqueous solution onto NaOH-modified rice husk. Carbohydr Polym. 2011;86(4):1533–41.
17. Saha P Das, Chakraborty S, Das S. Optimization of hazardous crystal violet by chemically treated rice husk: Using central composite response surface methodology. Arch Env Sci. 2012;6:57–61.
18. Masoumi A, Hemmati K, Ghaemy M. Low-cost nanoparticles sorbent from modified rice husk and a copolymer for efficient removal of Pb(II) and crystal violet from water. Chemosphere. 2016;146:253–62.
19. Luyen NT, Linh HX, Huy TQ. Preparation of Rice Husk Biochar-Based Magnetic Nanocomposite for Effective Removal of Crystal Violet. J Electron Mater. 2020;49(2):1142–9.
20. Chowdhury S, Chakraborty S, Saha P Das. Response surface optimization of a dynamic dye adsorption process: A case study of crystal violet adsorption onto NaOH-modified rice husk. Environ Sci Pollut Res. 2013;20(3):1698–705.
21. Peres EC, Favarin N, Slaviero J, Almeida ARF, Enders MP, Muller EI, et al. Bio-nanosilica obtained from rice husk using ultrasound and its potential for dye removal. Mater Lett. 2018;231:72–5.
22. Islam T, Liu J, Shen G, Ye T, Peng C. Synthesis of chemically modified carbon embedded silica and zeolite from rice husk to adsorb crystal violet dye from aqueous solution. Appl Ecol Environ Res. 2018;16(4):3955–67.
23. Flaih EH, Ali SA, Kadhim SH. Removal and electrochemical investigation of crystal violet dye in aqueous solutions by using rice husk treated with succinic acid. Int J Pharm Res. 2020;12(2):466–73.
24. Madhamshettiwar S V. A Study on Adsorption Process by Activated Rice Husk by Using Crystal Violet as Dye by Spectrophotometric Method Introduction : 442402:284–91.
25. Jain S, Jayaram R V. Removal of basic dyes from aqueous solution by low-cost adsorbent: Wood apple shell (Feronia acidissima). Desalination. 2010;250(3):921–7.
26. Motulsky HJ, Ransnas LA. Fitting curves to data using nonlinear regression: a practical and nonmathematical review. FASEB J. 1987;1(5):365–74.
27. Dan-Iya BI, Shukor MY. Isothermal Modelling of the Adsorption of Chromium onto Calcium Alginate Nanoparticles. J Environ Microbiol Toxicol. 2021;9(2):1–7.
28. Khare KS, Phelan FR. Quantitative Comparison of Atomistic Simulations with Experiment for a Cross-Linked Epoxy: A Specific Volume-Cooling Rate Analysis. Macromolecules. 2018;51(2):564–75.
29. Halmi MIE, Ku Ahamad KE, Shukor MY, Wasoh MH, Abdul Rachman AR, Sabullah MK, et al. Mathematical modelling of the degradation kinetics of Bacillus cereus grown on phenol. J Environ Bioremediation Toxicol. 2014;2(1):1–8.
30. Langmuir I. THE ADSORPTION OF GASES ON PLANE SURFACES OF GLASS, MICA AND PLATINUM. J Am Chem Soc. 1918;40(2):1361–402.
31. Schirmer W. Physical Chemistry of Surfaces. Z Für Phys Chem. 1999;210(1):134–5.
32. Ridha FN, Webley PA. Anomalous Henry's law behavior of nitrogen and carbon dioxide adsorption on alkali-exchanged chabazite zeolites. Sep Purif Technol. 2009;67(3):336–43.
33. Jovanović DS. Physical adsorption of gases - I: Isotherms for monolayer and multilayer adsorption. Kolloid-Z Amp Z Für Polym. 1969;235(1):1203–13.
34. Carmo AM, Hundal LS, Thompson ML. Sorption of hydrophobic organic compounds by soil materials: Application of unit equivalent Freundlich coefficients. Environ Sci Technol. 2000;34(20):4363–9.
35. Temkin MI, Pyzhev V. Kinetics of ammonia synthesis on promoted iron catalysts. Acta Physicochim USSR. 1940;12(3):327–56.
36. Radushkevich LV. Potential theory of sorption and structure of carbons. Zhurnal Fiz Khimii. 1949;23:1410–20.
37. Dubinin MM. Modern state of the theory of volume filling of micropore adsorbents during adsorption of gases and steams on carbon adsorbents. Zh Fiz Khim. 1965;39(6):1305–17.
38. Redlich O, Peterson DL. A Useful Adsorption Isotherm. Shell Dev Co Emeryv Calif. 1958;63:1024.
39. Sips R. On the structure of a catalyst surface. J Chem Phys. 1948;16(5):490–5.
40. Tóth J. Uniform interpretation of gas/solid adsorption. Adv Colloid Interface Sci. 1995;55(C):1–239.
41. Khan AA, Singh RP. Adsorption thermodynamics of carbofuran on Sn (IV) arsenosilicate in H+, Na+ and Ca2+ forms. Colloids Surf. 1987;24(1):33–42.
42. Brunauer S, Emmett PH, Teller E. Adsorption of Gases in Multimolecular Layers. J Am Chem Soc. 1938;60(2):309–19.
43. Vieth WR, Sladek KJ. A model for diffusion in a glassy polymer. J Colloid Sci. 1965;20(9):1014–33.
44. Radke CJ, Prausnitz JM. Adsorption of Organic Solutes from Dilute Aqueous Solution of Activated Carbon. J Am Chem Soc. 1972;11(4):445–51.
45. Gregg SJ, Sing KSW. Adsorption, surface area, and porosity. London: Academic Press; 1991. 328 p.
46. Fritz W, Schluender EU. Simultaneous adsorption equilibria of organic solutes in dilute aqueous solutions on activated carbon. Chem Eng Sci. 1974;29(5):1279–82.
47. Baudu M. Etude des interactions solute–fibres de charbon actif. Application et regeneration. Universite de Rennes I; 1990.
48. Parker Jr. GR. Optimum isotherm equation and thermodynamic interpretation for aqueous 1,1,2-trichloroethene adsorption isotherms on three adsorbents. Adsorption. 1995;1(2):113–32.

49. van Vliet BM, Weber Jr WJ, Hozumi H. Modeling and prediction of specific compound adsorption by activated carbon and synthetic adsorbents. Water Res. 1980;14(12):1719–28.
50. Burnham KP, Anderson DR. Multimodel inference: Understanding AIC and BIC in model selection. Sociol Methods Res. 2004;33(2):261–304.
51. Akaike H. A New Look at the Statistical Model Identification. IEEE Trans Autom Control. 1974;19(6):716–23.
52. Daifullah AAM, Girgis BS, Gad HMH. Utilization of agro-residues (rice husk) in small waste water treatment plans. Mater Lett. 2003;57(11):1723–31.
53. Abdelwahab O, Nemr A El, El-Sikaily A, Khaled A. Use of rice husk for adsorption of direct dyes from aqueous solution: A case study of direct F. Scarlet Green synthesis of TiO2 nanoparticles and its toxicity View project Industrial valorization of local biological materials and wastes for wastewater tre. Egypt J Aquat Res. 2005;31(May).
54. Della VP, Kühn I, Hotza D. Caracterização de cinza de casca de arroz para uso como matéria-prima na fabricação de refratários de sílica. Quimica Nova. 2001;24(6):778–82.